





# Effect of Natural Degradation on Wood Samples Used in Late Ottoman Period Architecture: A Case Study from Kahramanmaraş (Southern Türkiye)

Oktay Dumankaya <sup>a,\*</sup> Gonca Düzkale Sözbir <sup>b</sup> Songül Şahin Dumankaya <sup>c</sup> and Tamer Sözbir <sup>d</sup>

This article examines the chemical deterioration of wooden materials on the exterior surfaces of a historical mansion in Kahramanmaraş, constructed using the Bağdadi Wall Construction Technique, which is a rare example of Late Ottoman-Turkish architecture. The study employed various analyses to demonstrate that environmental factors, such as air, temperature, light, rain, and biological decay, have aged the wood. Fourier transform infrared analysis revealed a decrease in holocellulose peak density and lignin degradation. X-ray diffraction analysis indicated that the amorphous components of hardwood had diminished, leading to an increase in crystallinity, while the crystalline cellulose content in softwood had decreased, thereby weakening the structure. Thermal analysis uncovered changes in thermal stability between the wood's outer and inner surfaces. Ultraviolet analysis indicated a 21% color change on the exterior compared to that in the interior. Despite the deterioration of the exterior, the interior surfaces remained intact. Appropriate measures could prolong the mansion's lifespan, and urgent restoration is necessary to preserve this important cultural heritage.

DOI: 10.15376/biores.20.2.3424-3442

*Keywords:* FTIR; XRD; TGA/DTG/DTA; UV analyses; Late Ottoman period; Cultural heritage; Ottoman-Turkish house

*Contact information:* a: Department of Archaeology, Faculty of Humanities and Social Science, Kahramanmaraş Sütçü İmam University, Türkiye; b: Vocational School of Technical Sciences, Kahramanmaraş Sütçü İmam University, Türkiye; c: Department of Materials Science and Engineering, Kahramanmaraş Sütçü İmam University, Türkiye; d: Kahramanmaraş Paper Industry Inc., Türkiye; \* Corresponding author: oktaydumankaya@gmail.com

## INTRODUCTION

Kahramanmaraş is located on significant trade routes connecting ancient Anatolian geography and is positioned at the intersection of trade routes extending from Syria and Mesopotamia to Anatolia. Dating back to the 3<sup>rd</sup> millennium BCE, the city hosted various civilizations, such as the Hittites and Gurgum during the Neo-Hittite period, Antiocheia and Taurum in the Hellenistic period, and Caesarea Germanicia in the Roman period (Ürkmez 2014; Dumankaya 2019; Yıldırım and Kalaycı 2022, 2023). Furthermore, it accommodated the Byzantine, Seljuk, and Ottoman civilizations. Kahramanmaraş' center contains many remnants of ancient cultures, including examples of Ottoman-Turkish houses representing the Ottoman period.

The terms “Turkish house,” “Ottoman house,” and “Anatolian house,” are commonly used to refer to traditional Ottoman-Turkish houses. Especially in Istanbul, the

capital of the Ottoman Empire, the most exquisite examples of Ottoman-Turkish houses can be found. The development and spread of Ottoman-Turkish houses in Anatolia took place mainly during the 17<sup>th</sup> and 18<sup>th</sup> centuries (Gabriel 1938). Over time, Ottoman-Turkish houses spread to a vast geography including the Balkans, the Caucasus, the Caspian region, and Crimea, where suitable building materials were readily available. Traditional Turkish houses were typically constructed using natural materials such as stone, adobe, and wood. Local architecture is characterized by the use of local materials with low embodied energy, and thus minimal environmental impact, alongside environmental adaptation in terms of local climate conditions and topography (Philokyrou and Michael 2020; Durak and Ayyıldız 2023). Wood has remained a favored material in traditional architecture due to its natural properties. Its easy availability, workability, and ease of handling, combined with superior performance under loads, made it an essential choice for construction. Especially in Anatolia, where earthquakes are frequent, the flexibility of wood has played a crucial role in enhancing the earthquake resistance of buildings (Aksoy and Ahunbay 2010). However, starting from the 20<sup>th</sup> century, Ottoman-Turkish houses gradually began to be replaced by reinforced concrete buildings (Eldem 1954, 1984; Burkut 2019; Karakuş 2021).

In Kahramanmaraş, although there are examples of traditional Ottoman-Turkish houses preserved to this day through simple repairs, deteriorations in the wooden sections have been observed. In this study, chemical deteriorations in the wooden materials used in the mansion constructed in the first quarter of the 19<sup>th</sup> century Ottoman-Turkish architecture located in Turan Neighborhood, Dulkadiroğlu district of Kahramanmaraş, at parcel 45 of block 1736 (formerly numbered 465), have been examined, and recommendations for necessary measures have been provided.



**Fig. 1.** View of the Historic Turkish Mansion

The mentioned structure is located within the boundaries of the Dulkadiroğlu district. Situated on the slopes of a prominent hill, approximately 400 m from the Kahramanmaraş Castle, it represents one of the finest examples of Late Ottoman Period architecture. The ground floor of the structure is built using a stone masonry system, while the walls of the rooms are constructed with the “Baghdadi wall construction technique”. In the Baghdadi wall construction technique, wooden slats are horizontally placed at regular intervals on a wooden frame. The dimensions of the slats used in this technique are typically  $10 \times 12 \text{ cm}^2$ , with a thickness of 1.5 cm to 2 cm, and a width of 2.5 cm to 3.5 cm. The slats are plastered with lime mortar on both the interior and exterior surfaces (Erman 2000; Tayla 2007). The timber material used in the wall construction has a fibrous and porous structure, which despite being lightweight, demonstrates high strength due to these characteristics (Eriç 1978). However, significant deterioration is observed in the timber frame walls constructed using the Baghdadi technique. Additionally, the timber columns supporting the roof have collapsed, leading to the roof’s failure (Fig. 1). Based on its architectural and structural features, the building is believed to have been constructed in the late 19<sup>th</sup> century.



**Fig. 2.** The locations from which the wooden samples were extracted are as follows: A) The first sample was taken from the wooden ceiling of the ground floor; B) The second wooden sample was taken from the timber frame

Two samples were extracted from the mentioned structure for analysis, ensuring they were derived from the original wooden components of the building. The first sample



was obtained from the roofing planks of the second floor, while the second sample was taken from the wooden beams interspersed between the walls. The wood used for the roofing material and the beams between the walls is presumed to be from a coniferous tree species (Fig. 2).

Wood has been a crucial component in human life since historical times. Its fundamental composition includes cellulose, hemicellulose, and lignin polymers. When subjected to suitable conditions in the biological life cycle, wood undergoes structural deterioration (Eriksson and Johnsrud 1982; Björdal 2000). Factors such as sunlight, oxygen, water, heat, wind, pollution, and microorganisms lead to both intermolecular and intramolecular degradation of wood polymers, ultimately compromising its structural integrity. Solar radiation, particularly, induces photochemical degradation on the wood surface, primarily affecting lignin (Björdal 2000; Kranitz *et al.* 2016). Moisture content fluctuations resulting from rainfall or water exposure cause continual swelling and shrinking of the wood cell wall, thereby increasing the formation of cracks (Hosseinpourpia *et al.* 2018). While temperature may not be as critical as humidity and sunlight, higher temperatures accelerate photochemical, oxidative reactions, and wood decay rates (Feist 1990; Ghavidel *et al.* 2020a, 2020b). Enzymes from fungi play a crucial role in extensively breaking down cellulose and hemicellulose units, which are responsible for wood material strength (Koike *et al.* 2009). Significant strength losses and the formation of cubic cracks occur in the early stages of decay (Green and Highley 1997). Brown-rot fungi, particularly prevalent in damp, warm, and windless environments, commonly affect old and historical building woods (Jennings and Bravery 1991; Watkinson and Eastwood 2012).

X-ray diffraction (XRD), particularly present in lignocellulosic materials, such as wood, exhibits a certain degree of cellulose crystallinity due to the presence of free hydroxyl groups in the cellulose macromolecules, which participate in different intramolecular and intermolecular hydrogen bonding arrangements (Broda and Carmen-Mihaela 2019). The crystallinity of wood has a significant impact on the physical, mechanical, and chemical properties of wood-based materials. For instance, as crystallinity increases, the Young's modulus, tensile strength, dimensional stability, density, and hardness increase, while moisture regain, paint absorption, chemical reactivity, swelling, and flexibility decrease. Therefore, determining the crystallinity of wood could be an approach to understanding the effect of environmental conditions on wood properties. However, the complex chemical composition, texture, and highly anisotropic structure of wood make the determination of crystallinity challenging. The XRD and Fourier transform infrared (FTIR) spectroscopy have been utilized to monitor changes in wood crystallinity induced by chemical and biological degradation (Howell *et al.* 2009; Fackler *et al.* 2011), although they do not provide reliable absolute values of crystallinity but rather relative values (Park *et al.* 2010).

The thermogravimetric analysis (TGA)/derivative thermogravimetric (DTG) analyses provide information about the thermal stabilities of the components constituting wood (Skreiberg *et al.* 2011; Zhou *et al.* 2013). The organic components in cellulose, hemicellulose, and lignin, the main constituents of wood, react to environmental conditions. Photodegradation is the most rapid and potent event in the degradation of wood due to environmental effects (Hon and Chang 1984; Hon and Feist 1984). Particularly, lignin is the most sensitive wood component to photodegradation induced by ultraviolet (UV) light (Pandey 2005; Reinprecht 2016).

Wood can absorb electromagnetic radiation at several different wavelengths, initiating photochemical reactions that lead to the discoloration of wood. Wood contains

cellulose, hemicellulose, lignin, and extractive substances. All wood polymers are sensitive to ultraviolet radiation. Solar radiation depolymerizes lignin and cellulose, and water filters out the resulting photo-degraded fragments from the wood (Derbyshire and Miller 1981; Evans *et al.* 1993).

## EXPERIMENTAL

The portions of the samples obtained for chemical analysis from the wooden structures used in the roofing and beam elements of the historic mansion are provided below. Upon macroscopic examination of the wooden sample used in the roofing, the portions analyzed include the heavily degraded outer surface (E) and the undamaged inner surface (G). For the wooden beam sample, the portions analyzed include the heavily degraded outer surface (C) and the undamaged inner surface (D) (Fig. 3). For each sample, sections were taken from both the outer layer, where degradation was clearly visible (approximately 2 cm thick), and the core area of the wood.



**Fig. 3.** The analysis sections (internal - external) of the wooden samples (E, G, C, D)

The FTIR analysis (Attenuated Total Reflectance/ATR) was performed using a Shimadzu IRAffinity-1 FTIR instrument with 32 scans per sample and a resolution of  $4\text{ cm}^{-1}$  at wavelengths ranging from  $4000$  to  $800\text{ cm}^{-1}$ . For XRD, a Panalytical Philips X'Pert PRO XRD instrument was utilized under conditions of  $40\text{ kV}$  and  $30\text{ mA}$ , with monochromatic  $\text{CuK}\alpha$  radiation ( $\lambda = 0.154056\text{ nm}$ ). The XRD measurements were taken in the temperature range of  $10$  to  $100\text{ }^\circ\text{C}$  with a step interval of  $0.02\text{ }^\circ\text{C}$ , and each step was held for  $1\text{ s}$ . The crystallinity index (CrI) was calculated using Eq. 1 from Segal *et al.* (1959) internal reference method. In this formula,  $I_{002}$  represents the maximum intensity of the peak at  $2 \pm 22.5^\circ$ , and  $I_{am}$  corresponds to the intensity at  $2 \pm 18^\circ$ .

$$CrI (\%) = \left[ \frac{I_{002} - I_{am}}{I_{002}} \right] \times 100 \quad (1)$$

The wood samples were subjected to differential thermal analysis using the Perkin Elmer, Diamond TG/DTA – Seiko Instruments SII, Exstar 6300 TG/DTA. The analysis was conducted in a nitrogen atmosphere within the temperature range of  $30$  to  $800\text{ }^\circ\text{C}$ . For UV analysis, the samples were examined using the HunterLab Color Flex device under D65 daylight and a  $10\text{ }^\circ\text{C}$  viewing angle to assess color changes based on  $L^*$ ,  $a^*$ , and  $b^*$  values. The total color difference ( $\Delta E^*$ ) was calculated, with  $\Delta E^*$  measured on a scale

from 0 to 100; where 0 indicates minimal color change and 100 signifies complete deterioration.

## RESULTS AND DISCUSSION

When the FTIR analysis of the C and D sections of the wooden samples obtained from the historic mansion was examined, an asymmetric stretching vibration peak of methyl and methylene groups located in cellulose, hemicellulose, and lignin was obtained at the wavelength of  $3321\text{ cm}^{-1}$  (Faix 1992; Pandey and Pitman 2003; Carrillo *et al.* 2004; Schwanninger *et al.* 2004; Bodirlau and Teaca 2009). At the wavelength of  $2917\text{ cm}^{-1}$ , symmetric stretching vibrations of methyl and methylene groups present in holocellulose were detected (Pandey and Pitman 2003; Carrillo *et al.* 2004; Schwanninger *et al.* 2004). A vibration peak related to the stretching of C=C and C=O groups in the lignin structure was identified at the wavelength of  $1621\text{ cm}^{-1}$  (García-Iruela *et al.* 2020; Ghavidel *et al.* 2020a). At the wavelength of  $1262\text{ cm}^{-1}$ , the C-O stretching vibration of guaiacyl lignin ring and the -OH and -CH bending vibrations of the holocellulose unit were determined. The stretching vibration peaks of C-O and C-C in holocellulose were obtained at the wavelength of  $1019\text{ cm}^{-1}$  (Faix 1992; Pucetaite 2012; Pedersen *et al.* 2021) (Fig. 4).

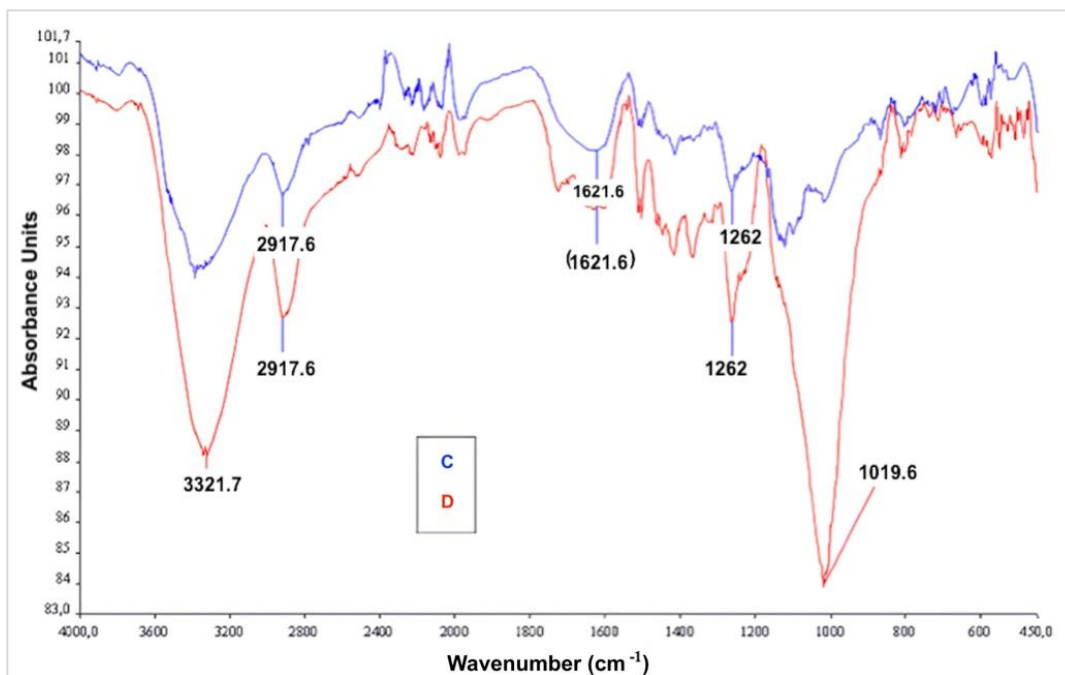


**Fig. 4.** The FTIR graphs of the C and D sections of the wooden samples

Upon comparison of the outer surface (C) of the wooden samples with the inner surface (D), where degradation was less or absent, it was observed that the intensity of the peak decreased at the wavelength region of  $800\text{ to }900\text{ cm}^{-1}$ . These wavelengths are related to the cellulose content of the wood (Derbyshire and Miller 1981; Hoffmann and Jones 1990). A significant peak loss was detected at the wavelength of  $1019\text{ cm}^{-1}$ , clearly indicating the loss of holocellulose in the wood. There was a decrease in peak intensity between wavelengths of  $1250\text{ and }1500\text{ cm}^{-1}$ . This decrease was associated with the lignin

content, and on this surface (C), where degradation is more pronounced, lignin degradation was observed.

In a study examining archaeological wood samples using FTIR analysis, the loss at wavelengths of  $1235\text{ cm}^{-1}$  and  $1646\text{ cm}^{-1}$  was attributed to the vibrations of the C=O and C=C groups in the lignin structure (Ghavidel *et al.* 2021a, 2021b). A peak loss was identified at  $1700\text{ cm}^{-1}$ , which is associated with hemicellulose component (Ljungdahl and Eriksson 1985; Lucejko *et al.* 2020; High and Penkman 2020). A decrease in intensity was determined at  $3320\text{ cm}^{-1}$ , indicating a reduction in holocellulose content at this wavelength (Fig. 4).

The stretching vibration in the region between  $2800$  and  $3000\text{ cm}^{-1}$  is associated with the –CH group in cellulose, hemicellulose, and lignin (Ghavidel *et al.* 2020a, 2020b). The band at  $1733\text{ cm}^{-1}$ , assigned to the stretching vibrations of non-conjugated C=O groups and specific regions, was missing in the wood samples. This may be associated with the significant degradation of hemicellulose after the aging process (Ljungdahl and Eriksson 1985; Lucejko *et al.* 2020; High and Penkman 2020).

When the FTIR analysis of the E and G sections (Fig. 5) was examined, peaks of O-H stretching vibrations originating from cellulose and hemicellulose content were detected at wavelengths of  $3357$  to  $3340\text{ cm}^{-1}$ . At  $2912\text{ cm}^{-1}$  wavelength, the peak of asymmetric stretching vibrations of methyl and methylene-bound C-H stretchings in cellulose, hemicellulose, and lignin were obtained. At  $1599$  and  $1503\text{ cm}^{-1}$ , peaks due to stretching vibrations in the aromatic structure of the lignin component were found (Pucetaite 2012; Emmanuel *et al.* 2015; Moosavinejad *et al.* 2016). At  $1415\text{ cm}^{-1}$ , a peak of vibrations in the aromatic structure within lignin was observed (Pandey and Pitman 2020). At  $1264\text{ cm}^{-1}$ , the stretching vibrations of C-O in guaiacyl ring in lignin and the swinging peaks of OH and CH in hemicellulose were obtained. At  $1021\text{ cm}^{-1}$  wavelength, peaks of stretching vibrations of C-O and C-C in hemicellulose were obtained (Faix 1992; Pucetaite 2012).

In the E samples with degraded outer surfaces, the peak of OH vibrations originating from hemicellulose and cellulose content at  $3340\text{ cm}^{-1}$  was found more intensely in the G samples obtained from the more intact inner surfaces at  $3357\text{ cm}^{-1}$ . This is thought to be due to the brown-rot fungi damaging the outer surfaces of the wood, and additionally, photodegradation occurring on the outer surfaces. The peak of C=C stretching vibrations in the aromatic structure within lignin observed at  $1594\text{ cm}^{-1}$  in the E samples was found to be more intense at  $1599\text{ cm}^{-1}$  wavelength in the G sample with intact wood. This is believed to be due to photodegradation occurring on the outer surfaces of the wood affecting the lignin content.

At  $1415\text{ cm}^{-1}$ , a peak of vibrations in the aromatic structure within lignin was obtained in the E samples, which is not observed in the G samples. This peak is the vibrational peak associated with the aromatic structure in the lignin content. It is thought to be intensely observed on degraded surfaces due to the reduction in the hemicellulose content in the wood caused by the damage inflicted by brown rot fungi, which consequently leads to a relative increase in lignin content.

Between wavelengths of  $1050$  and  $1100\text{ cm}^{-1}$ , the peak intensity decreased on the outer surfaces (E) with intact degradation. The reason for this may be that while the peak of C-C and C-O vibrations in hemicellulose content was observed in the sample taken from the inner surface (G) at these wavelengths, the intensity decreased in the degraded outer surfaces (E). This is attributed to photodegradation and the action of brown rot fungi on the wood's outer surfaces.



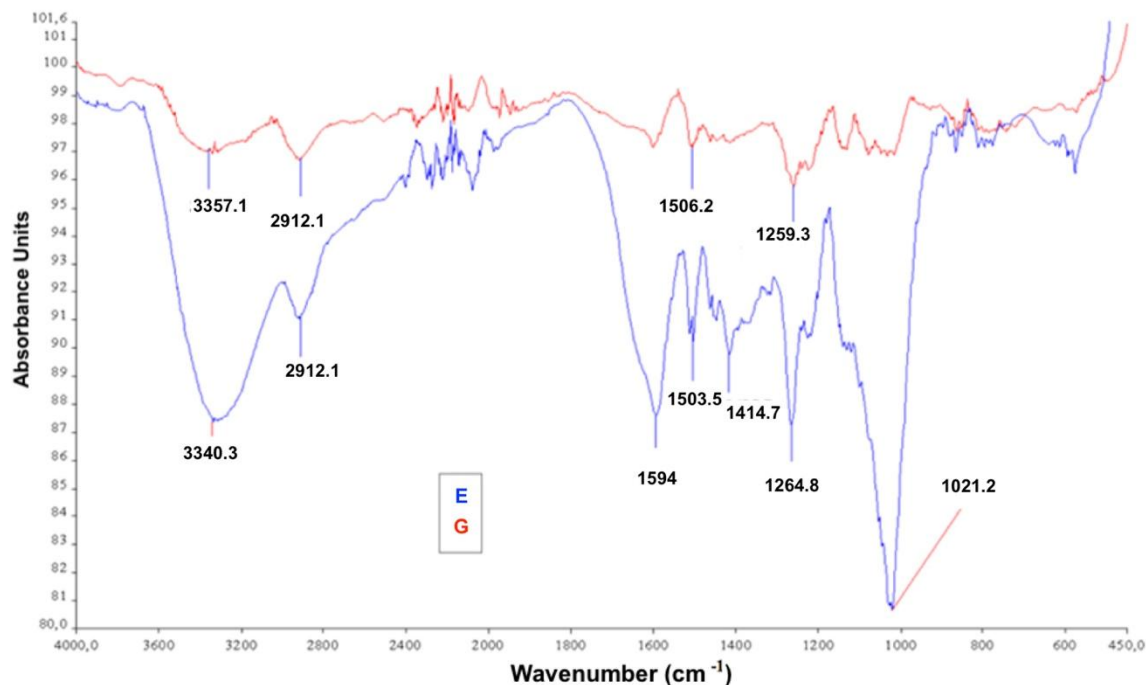


**Fig. 5.** The FTIR graphs of the E and G sections of the wooden samples

When comparing the outer surface (C) and the less degraded inner surface (D) of the wooden samples, the crystallinity index of the outer surface (C) was determined to be 65%, while the crystallinity index of the inner surface was determined to be 55% (Fig. 6).

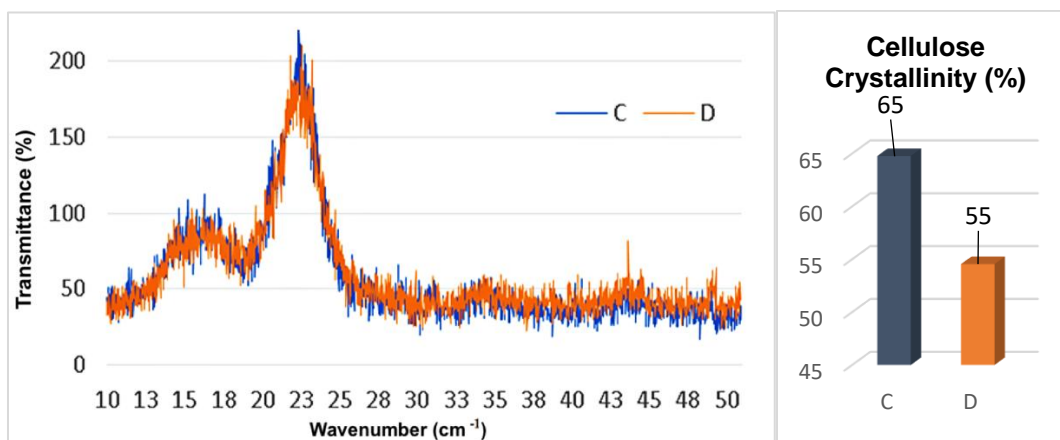


**Fig. 6.** The XRD graphs of the C and D sections of the wooden samples

The reason for the increase in crystallinity index on the outer surface is believed to be the action of microorganisms, especially those causing degradation in wood materials. This may lead to the increase in crystallization of the wood component due to the degradations of lignin and hemicellulose, which have an amorphous structure (Howell *et al.* 2009). It is considered that substantial changes in crystallinity index and crystallite size may lead to an increase in the relative ratio of crystalline wood components after the removal of the amorphous fractions (lignin and hemicellulose). In this study, the samples



are estimated to be from hardwood. In a study, the crystallinity of poplar wood was determined to be 60.6% (Gu *et al.* 2019). Although it is evident that the inner surface of the wood is less degraded compared to the outer surface, this does not necessarily mean that the inner surface of the wood has not degraded at all over the years. A study has found that environmental conditions and decay factors over time reduce the crystallinity index of wood (Bouramdane *et al.* 2022).

When comparing the outer surface (E) and the less degraded inner surface (G) of the wooden samples, the crystallinity index of the outer surface (E) was determined to be 42%, while the that of the inner surface (G) was determined to be 45% (Fig. 7). It is presumed that the examined tree species is coniferous wood. In a study examining the degradation of wood under outdoor conditions, it was found that the crystallinity index of cellulose decreased due to the influence of outdoor conditions. They reported that wood cellulose was initially crystalline and that environmental degradation conditions made the wood more amorphous (Kim and Kuga 2001; Bouramdane *et al.* 2022). Additionally, they found that the loss of crystallinity was due to the opening of glycopyranose rings and the disruption of the regular structure (Kim and Kuga 2001; Li *et al.* 2011). The decrease in wood crystallinity during degradation processes under outdoor conditions indicates a reduction in hydrogen bonds in crystalline cellulose when temperature or oxidation levels increase. As a result, cellulose microfibrils become stiffer and more brittle, leading to a significant breakdown of hydrogen bonds and thus a cellulose structure that is easily degraded (Bouramdane *et al.* 2022).

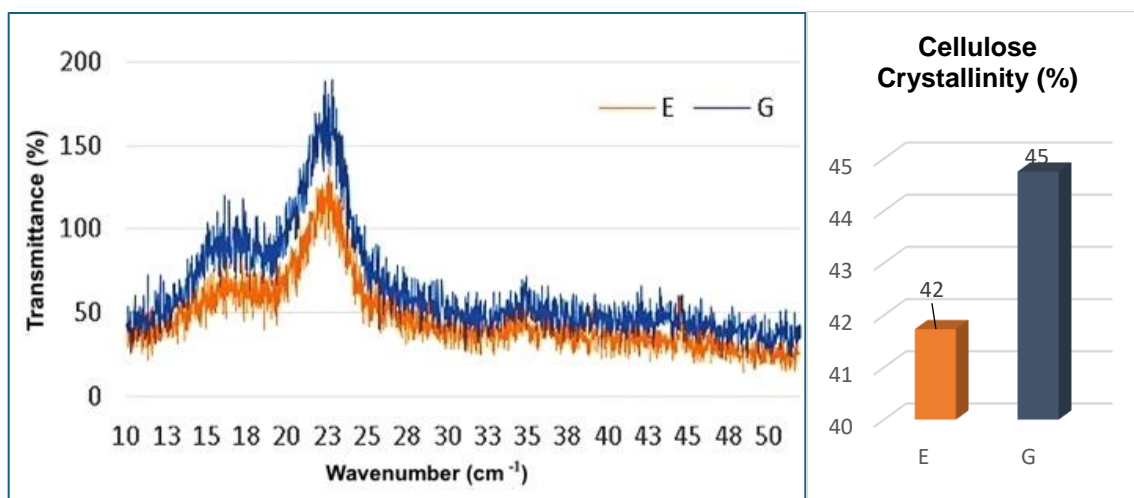
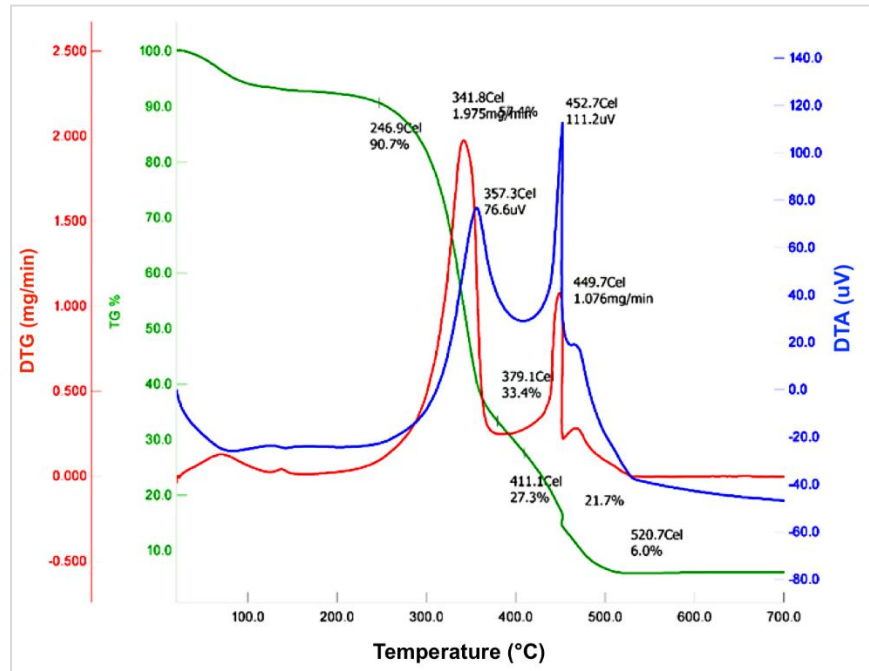


Fig. 7. The XRD graphs of the E and G sections of the wooden samples

In the TGA, DTG, and DTA analyses of the D and C samples, the D samples (inner surface) started to degrade at 261 °C, and degradation reaction was completed at 499 °C (Figs. 8 and 9). It was determined that two exothermic reactions occurred during the degradation reaction, and at the beginning of the first degradation reaction, there was 89.6% substance, while the reaction started with 16.8% substance at the beginning of the second reaction. 72% of the substance was degraded between the two reactions. About 3.3% of the substance remained after the combustion reaction. The highest weight loss in the first reaction occurred at 352 °C with a rate of 2.151 mg/min, while in the second degradation occurred at 454 °C with a rate of 1.309 mg/min. The C sample (outer part) started to degrade at 246 °C and ended at 520.7 °C. Two exothermic reactions occurred

during the degradation process. At the beginning of the first degradation reaction, there was 90.7% substance, while the reaction started with 27.3% substance at the beginning of the second reaction. 63.4% of the substance was degraded between the two reactions. 6% of the substance remained after the reaction. It was determined that the weight loss rate of the D sample was higher than that of the C sample in both reactions.



**Fig. 8.** The TGA, DTG, and DTA graphs of the C sections of the wooden samples

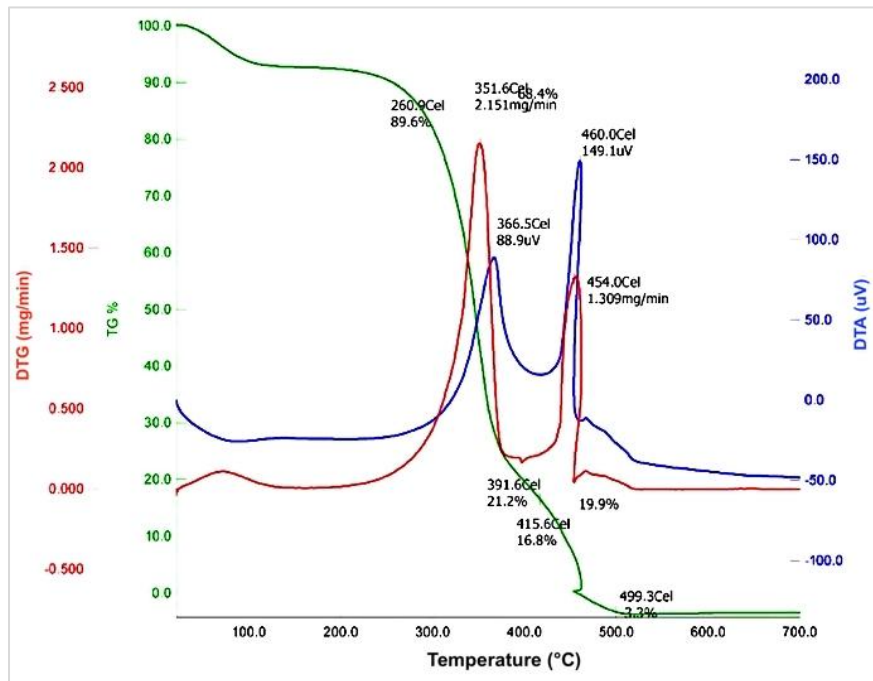


**Fig. 9.** The TGA, DTG, and DTA graphs of the D sections of the wooden samples

Upon examination of the TGA, DTG, and DTA graphs of the E and G samples (Figs. 10 and 11), it is apparent that the degradation reaction of sample G began at 239 °C and was completed at 489 °C. At the end of the degradation reaction, 0% of the substance remained. The degradation involved two exothermic reactions. The first exothermic reaction of the G sample occurred at the highest temperature of 333.7 °C, with a degradation rate of 1.995 mg/min, while the second degradation reaction occurred at the highest temperature of 429 °C, with a rate of 0.829 mg/min. At the end of the reaction, 0% of the substance remained.

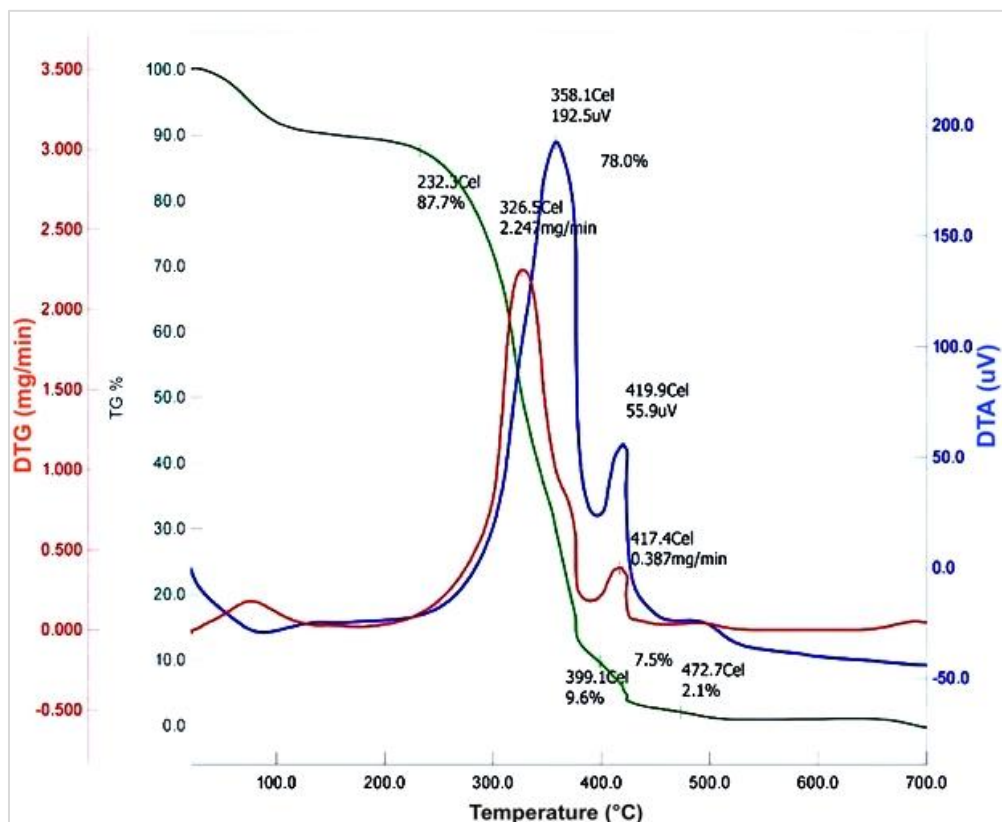


Fig. 10. The TGA, DTG, and DTA graphs of the E of the wooden samples

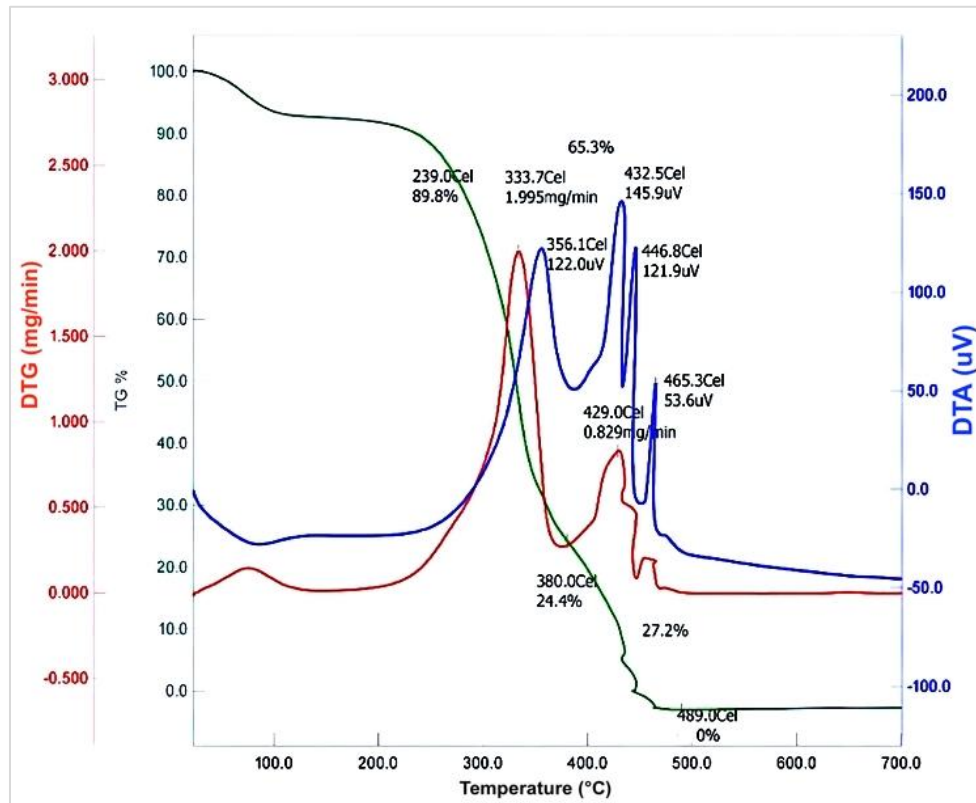


Fig. 11. The TGA, DTG, and DTA graphs of the G of the wooden samples

According to the TGA, DTG, and DTA graphs of the E sample, the degradation reaction began at 232.3 °C and was completed at 399 °C. The reaction occurred in two stages as exothermic. At the end of the reaction, 2.1% of the substance remained. The first exothermic reaction of the E samples occurred at the highest temperature of 326.5 °C, with a degradation rate of 2.247 mg/min, while the second degradation reaction occurred at the highest temperature of 417 °C, with a rate of 0.387 mg/min. It was observed that the weight loss rate of the E samples was higher in the first exothermic reaction, while it was higher for the G samples in the second exothermic reaction.

Upon examination of the E and G samples, it was observed that the starting and completion temperatures of the degradation reaction due to thermal effects were lower for the E samples, which are more exposed to degradation under outdoor conditions, compared to the inner part (G), indicating a decrease in the thermal stability of the wooden samples.

When examining the D-C and E-G sections of wooden samples taken from two different locations in the historical mansion, it was observed that the initiation and completion temperatures of the degradation reaction because of temperature were lower for the C and E samples, which were more exposed to environmental degradation, compared to the inner parts. Thus, it was determined that the thermal resistance of the wooden samples decreased. When the weight loss rates were analyzed, it was found that the weight loss rates of the inner surface of the wood were higher than those of the degraded outer surface. This is because the outer surface of the wood is particularly affected by wood decay and undergoes structural changes. It is evident that the outer surface of the wood is exposed to brown decay due to the formation of brown cracks. Brown decay primarily consumes holocellulose from the components of wood, causing less damage to the lignin content (Hill 2006). Therefore, the holocellulose content of the degraded outer surface



samples C and E had decreased over time. As a result, it was observed that the combustion rate was higher for the D and G samples, which have a higher holocellulose content. It was determined that the remaining substance in the C and E samples after the completion of the reaction was higher. This is thought to be due to the carbonization of the wood as a result of being more exposed to environmental conditions.

In this study, it was found that the shape of the DTG curves decreased the peak temperatures assigned to the evaporation of hemicelluloses and amorphous cellulose depending on the exposure time of the wood to *C. globosum* fungus. The shift to lower temperatures is attributable to the formation of oxidized structures after enzymatic degradation, making the wood less thermally stable (Popescu *et al.* 2010). In another study, it was found that the remaining ash content after the combustion of wood samples decayed by fungi was higher compared to intact wood (Kawase 1962).

In Table 1 it is observed that the total color change between the inner (D) and outer (C) surfaces of the wooden samples due to natural aging was 20.73%. Similarly, when analyzing the color change of other wooden samples obtained from the same location (Table 2), the total color change between the inner (G) and outer (E) surfaces of the wood was determined to be 21.25%.

**Table 1.** UV Analysis Results for Samples C and D

Sample	$L^*$	$a^*$	$b^*$
G	69.85	7.81	31.11
E	49.85	10.01	26.14
<b>Aging Difference</b>	20	-2.2	4.97
<b><math>\Delta E^*</math></b>		20.73	

When comparing the outer and inner surfaces of wood, it has been observed that both types of wood undergo photodegradation. In addition to the decrease in methoxyl and lignin contents and the increase in carboxyl content within the wood (Leary 1968), photodegradation also leads to an increase in cellulose content and a decrease in lignin content on the wood surface (Wang and Lin 1991; George *et al.* 2005). Considering other decay factors, this condition results in a reduction in some physical, chemical, and biological properties of natural wood.

**Table 2.** UV Analysis Results for Samples E and G

Sample	$L^*$	$a^*$	$b^*$
D	61.15	10.48	32.98
C	42.03	10.16	23.72
<b>Aging Difference</b>	19.12	0.32	9.26
<b><math>\Delta E^*</math></b>		21.25	

## CONCLUSIONS AND RECOMMENDATION

1. The results from the analysis on wood samples obtained from the historical mansion indicate that the wood has undergone aging due to environmental factors such as air, temperature, light, rain, and biological decay agents.
2. Based on the Fourier transform infrared (FTIR) analysis, it was understood that the peak density of hemicellulose responsible for the mechanical strength of the wood decreased, and lignin was degraded. According to the X-ray diffraction (XRD) analysis, it was found that in both hardwood and softwood, the amorphous components decreased, leading to an increase in the proportional crystallinity in hardwood and a decrease in the crystalline cellulose content in softwood, disrupting both the crystalline and amorphous regions of the wood structure.
3. The thermogravimetric analysis / differential thermal gravimetric / differential thermal (TGA/DTG/DTA) analyses indicated changes in thermal stability between the outer and inner surfaces of the wood. Furthermore, the ultraviolet (UV) analysis revealed that the color of the wood's outer surface changed approximately 21% compared to its inner part in both types of wood. As a result of the analyses, it is evident that the outer surfaces of the wood samples taken from the historic mansion had deteriorated, while the inner surfaces remain intact. With appropriate measures, such as conservation and restoration, the continued use of this structure is feasible.

The restoration and conservation of historic buildings are essential for ensuring the sustainability of cultural heritage. However, many structures have suffered significant damage due to neglect, improper interventions, and lack of knowledge (Ahunbay 2011; Akyıldız *et al.* 2016). During the restoration process, the mechanical, physical, and chemical properties of building materials such as stone, brick, wood, mortar, and plaster must be analyzed, and the reinforcement of the load-bearing system should be prioritized (Crocci 1998; Karakuş 2020). The stability of masonry walls, timber beams, columns, and connection points should be assessed, and reinforcement should be carried out using anchors, foundation underpinning, micropiles, and pile foundation systems to enhance the structure's resistance to settlement and seismic activity.

Among the commonly applied restoration and seismic strengthening techniques, Fiber Reinforced Polymers (FRP), cross-bracing, structural confinement, steel tie-bars, and reinforced concrete or steel plate jacketing are widely utilized (Karakuş 2019). To preserve the authenticity of the structure while ensuring its structural integrity, non-invasive, reversible, and minimally intrusive conservation solutions should be implemented in accordance with ICOMOS, UNESCO, and ASTM standards. A multidisciplinary approach integrating structural engineering, material science, and architectural conservation is crucial for maintaining the long-term stability and sustainability of historic buildings.

## REFERENCES CITED

- Aksoy, D., and Ahunbay, Z. (2010). "Geleneksel Ahşap İskeletli Türk Konutu'nun Deprem Davranışları [Seismic Behavior of Traditional Timber-Framed Turkish Houses]," *A/Z ITU Journal of the Faculty of Architecture/A* 4(1), 47-58.

- Akyıldız, M. H., Kesik, H. İ., Kubulay, Ç., Karamanoğlu, M., Bıçak, S., Olgun, Ç., and Tiftik, A. (2016). “Ahşap Malzeme Restorasyonunda Yüzey Temizleme Yöntemleri, [Surface cleaning methods in wood material restoration],” *Selcuk University Journal of Engineering Sciences (SUJES)* 2, 1100-1113.
- Björkdal, C. G. (2000). *Waterlogged Archaeological Wood, Biodegradation and Its Implications for Conservation*, Ph.D. Thesis, Swedish University of Agricultural Science, Uppsala, Sweden.
- Broda, M., and Carmen-Mihaela, P. (2019). “Natural decay of archaeological oak wood versus artificial degradation processes – An FT-IR spectroscopy and X-ray diffraction study,” *Spectrochimica Acta Part A: Molecular and Biomolecular Spectroscopy* 209, 280-287. DOI: 10.1016/j.saa.2018.10.057
- Bodirlau, R., and Teaca, C. A. (2009). “Fourier transform infrared spectroscopy and thermal analysis of lignocellulose fillers treated with organic anhydrides,” *Romanian Journal of Physics* 54(1-2), 93-104.
- Bouramdane, Y., Fellak, S., and El Mansouri, F. (2022). “Impact of natural degradation on the aged lignocellulose fibers of Moroccan cedar softwood: Structural elucidation by infrared spectroscopy (ATR-FTIR) and X-ray diffraction (XRD),” *Fermentation* 8(12), article 698. DOI: 10.3390/fermentation8120698
- Burkut, E. B. (2019). “Türk Evinin Mimari Özellikleri,” in: *Kültürel, Mimari ve Sosyal Hayatımızın Tanıkları: Türk Evleri [Witnesses of Our Cultural, Architectural, and Social Life: Turkish Houses]*, K. Alver, (ed.), Ümraniye Municipality Press, İstanbul, Türkiye, pp. 24-45.
- Carrillo, F., Colom, X., Suñol, Joan. J., and Saurina, J. (2004). “Structural FTIR analysis and thermal characterization of lyocell and viscose-type fibres,” *European Polymer Journal* 40(9), 2229-2234. DOI: 10.1016/j.eurpolymj.2004.05.003
- Croci, G. (1998). *The Conservation and Structural Restoration of Architectural Heritage*, Computational Mechanics Inc. UK and Boston, USA.
- Derbyshire, H., and Miller, E. R. (1981). “The photodegradation of wood during solar irradiation. Part 1: Effects on the structural integrity of thin wood strips,” *Holz RohWerkst* 39(8), 341-350.
- Dumankaya, O. (2019). “Kayıp Kent Germanicia: Lokalizasyon Problemleri Üzerine Yeni Gözlemler [The Lost City of Germanicia: New Observations on Localization Problems],” *Atatürk Üniversitesi Türkiyat Araştırmaları Enstitüsü Dergisi* 66, 409-434.
- Eldem, S. H. (1954). *Türk Evi Plan Tipleri [Types of Turkish House Plans]*, Pulhan Printing House, İstanbul, Türkiye.
- Eldem, S. H. (1984). *Türk Evi: Osmanlı Dönemi [Turkish Houses: Ottoman Period]*, Vol. I, T.A.Ç. Vakfı Güzel Sanatlar Printing House, İstanbul, Türkiye.
- Emmanuel, V., Odile, B., and Céline, R. (2015). “FTIR spectroscopy of woods: A new approach to study the weathering of the carving face of a sculpture,” *Spectrochimica Acta Part A: Molecular and Biomolecular Spectroscopy* 136, 1255-1259. DOI: 10.1016/j.saa.2014.10.011
- Eriç, M. (1978). *Yapı Malzemeleri [Building Materials]*, Vol. II, Kazmaz Press, İstanbul, Türkiye.
- Eriksson, K. E., and Johnsrud, S. C. (1982). “Mineralization of carbon,” in: *Experimental Microbial Ecology Burns*, G. B. Richard, and J. Howard-Slater (eds.), Blackwell, London, UK, pp. 134-153.

- Erman, E. (2000). "Bir Ahşap Yapı Kültürünün Yok Oluşu; Gölyaka [The destruction of a wooden construction culture: Gölyaka]," *ODTÜ MFD* 20(1-2), 57-76.
- Evans, P. D., Schmalzl, K. J., and Michell, A. (1993). "Rapid loss of lignin at wood surfaces during natural weathering," in: *Cellulosics: Pulp, Fibre and Environmental Aspects*, J. F. Kennedy, G. O. Phillips, and P. A. Williams, (eds.), Chichester, Ellis Horwood, UK, pp. 335-340.
- Durak, Ş., and Ayyıldız, S. (2023). "A model trial for the ecological evaluation of the traditional rural houses: Case of Yalova," *Journal of the Faculty of Engineering and Architecture of Gazi University* 38(1), 85-102.
- Fackler, K., Stevanic, J. S., Ters, T., Hinterstoisser, B., Schwanninger, M., and Salmén, L. (2011). "FT-IR imaging microscopy to localise and characterise simultaneous and selective white-rot decay within spruce wood cells," *Holzforschung* 65, 411-420. DOI: 10.1515/hf.2011.048
- Faix, O. (1992). "Fourier transform infrared spectroscopy," in: *Methods in Lignin Chemistry*, Stephan Y. Lin, and C. W. Dence (eds.), Berlin: Springer Berlin Heidelberg, Germany, pp. 83-109.
- Feist, W. C. 1990). "Outdoor wood weathering and protection," in: *Archaeological Wood: Properties, Chemistry, and Preservation, Advances in Chemistry Series* Roger M. Rowell, and J. Barbour (eds.), American Chemical Society, Washington, D.C., USA, pp. 263-298. DOI: 10.1021/ba-1990-0225.ch011
- Gabriel, A. (1938). "Türk Evi [Turkish house]," *Arkitekt* 89-90, 149-154.
- García-Iruela, A., García Esteban, L., García-Fernández, F., Palacios, P., Rodríguez-Navarro, A. B., Sánchez, L. G., and Hosseinpourpia, R. (2020). "Effect of degradation on wood hygroscopicity: The case of a 400-year-old coffin," *Forests* 11(7), article 712. DOI: 10.3390/f11070712
- George, B., Suttie, E., Merlin, A., and Deglise, X. (2005). "Photo degradation and photo stability of wood-the state of art," *Polymer Degradation & Stability* 88(2), 268-274. DOI: 10.1016/j.polymdegradstab.2004.10.018
- Ghavidel, A., Gelbrich, J., Kuqo, A., Vasilache, V., and Sandu, I. 2020a. "Investigation of archaeological European white elm (*Ulmus laevis*) for identifying and characterizing the kind of biological degradation," *Heritage* 3(4), 1083-1093. DOI: 10.3390/heritage3040060
- Ghavidel, A., Hofmann, T., Bak, M., Sandu, I., and Vasilache, V. (2020b). "Comparative archaeometric characterization of recent and historical oak (*Quercus* spp.) wood," *Wood Science and Technology* 54, 1121-1137. DOI: 10.1007/s00226-020-01202-4
- Ghavidel, A., Hosseinpourpia, R., Gelbrich, J., Bak, M., and Sandu, I. (2021a). "Microstructural and chemical characteristics of archaeological white elm (*Ulmus laevis* P.) and Poplar (*Populus* spp.)," *Journal of Applied Science* 11, article 10271. DOI: 10.3390/app112110271
- Ghavidel, A., Bak, M., Hofmann, T., Vasilache, V., and Sandu, I. (2021b). "Evaluation of some wood-water relations and chemometric characteristics of recent oak and archaeological oak wood (*Quercus robur*) with archaeometric value," *Journal of Cultural Heritage* 51, 21-28. DOI: 10.1016/j.culher.2021.06.011
- Green, F., and Highley, T. L. (1997). "Mechanism of brown-rot decay: Paradigm or paradox," *International Biodeterioration & Biodegradation* 39, 113-124. DOI: 10.1016/S0964-8305(96)00063-7
- Gu, Y., Bian, H., Wei, L., and Wang, R. (2019). "Enhancement of hydrotropic fractionation of poplar wood using autohydrolysis and disk refining pretreatment:



- Morphology and overall chemical characterization,” *Polymers* 11(4), article 685.  
DOI: 10.3390/polym11040685
- High, K. E., and Penkman, K. E. H. (2020). “A review of analytical methods for assessing preservation in waterlogged archaeological wood and their application in practice,” *Heritage Science* 8, article 83. DOI: 10.1186/s40494-020-00422-y
- Hill, C. (2006). *Wood Modification Chemical, Thermal and Other Processes*, Wiley & Sons Ltd., Hoboken, NJ, USA.
- Hoffmann, P., and Jones, M. A. (1990). “Structure and degradation process for waterlogged archaeological wood,” in: *Archaeological Wood*, American Chemical Society, Washington, D.C., USA, pp. 35-65.
- Hon, D. N., and Feist, W. C. (1984). “Chemistry of weathering and protection, in the chemistry of solid wood,” in: *Advances in American Chemical Society*, R. M. Rowell (ed.), Volume 27, ACS Publications, Washington, D.C., USA, pp. 401-451.
- Hon, D. N., and Chang, S. T. (1984). “Surface degradation of wood by ultraviolet light,” *Journal of Polymer Science: Polymer Chemistry Edition* 22(9), 2227-2241.  
DOI: 10.1002/pol.1984.170220923
- Hosseinpourpia, R., Adamopoulos, S., and Mai, C. (2018). “Effects of acid pre-treatments on the swelling and vapor sorption of thermally modified Scots pine (*Pinus sylvestris* L.) wood,” *BioResources* 13(1), 331-345. DOI: 10.15376/biores.13.1.331-345
- Howell, C., Steenkjaer-Hastrup, A. C., Goodell, B., and Jellison, J. (2009). “Temporal changes in wood crystalline cellulose during degradation by brown rot fungi,” *Journal of Polymer Science, Polymer Chemistry* 63, 414-419. DOI: 10.1016/j.ibiod.2008.11.009
- Karakuş, F. (2019). “Investigation of the repairing and strengthening methods in historical structures,” *International Journal of Scientific and Technological Research* 5(5), 81-98. DOI: 10.7176/JSTR/5-5-10
- Karakuş, F. (2020). “Analysis of the methods used in documentation of historical structures with examples,” *The Eurasia Proceedings of Science Technology Engineering and Mathematics* 11, 69-76.
- Karakuş, F. (2021). “A house in Ankara Ulucanlar district in the context of traditional Ottoman architecture,” *Journal of Art History* 30(2), 809-843. DOI: 10.29135/std.839302.
- Kawase, K. (1962). “Chemical components of wood decayed under natural condition and their properties,” *Journal of the Faculty of Agriculture* 52(2), 186-245.
- Kim, U. J., and Kuga, S. (2001). “Ion-exchange chromatography by dicarboxyl cellulose gel,” *Journal of Chromatography A* 919(1), 29-37. DOI: 10.1016/S0021-9673(01)00800-7
- Koike, K., Itakura, S., and Enoki, A. (2009). “Degradation of wood and enzyme production by *Ceriporiopsis subvermispora*, Author links open overlay panel Hiromi Tanaka,” *Enzyme and Microbial Technology* 45, 384-390. DOI: 10.1016/j.enzmictec.2009.06.003
- Kranitz, K., Sonderegger, W., Bues, C. T., and Niemz, P. (2016). “Effects of aging on wood: A literature review,” *Wood Science Technology* 50, 7-22. DOI: 10.1007/s00226-015-0766-0
- Leary, G. J. (1968). “Photochemical production of quinoid structures in wood,” *Nature* 217, 672-673. DOI: 10.1038/217672b0

- Li, H., Wu, B., Mu, C., and Lin, W. (2011). "Concomitant degradation in periodate oxidation of carboxymethyl cellulose," *Carbohydrate Polymers* 84(3), 881-886. DOI: 10.1016/j.carbpol.2010.12.026
- Ljungdahl, L. G., and Eriksson, K. E. (1985). "Ecology of microbial cellulose degradation," K. C. Marshall (ed.), in: *Advances in Microbial Ecology*, Vol. 8, Springer, Boston, MA, USA, pp. 237-299. DOI: 10.1007/978-1-4615-9412-3\_6
- Lucejko, J. J., Tamburini, D., Zborowska, M., Babinski, L., Modugno, F., and Colombini, M. P. (2020). "Oak wood degradation processes induced by the burial environment in the archaeological site of Biskupin (Poland)," *Heritage Science* 8(44), 1-12. DOI: 10.1186/s40494-020-00390-3
- Jennings, D. H., and Bravery, A. F. (1991). *Serpula Lacrymans: Fundamental Biology and Control Strategies*, Wiley, New York, NY, USA.
- Moosavinejad, S. S., Madhoushi, M., Rasouli, D., and Vakili, M. (2016). "Nondestructive evaluation of wood chemical compounds used in Gorgan historical building via FT-IR spectroscopy," *Journals of Forest Science and Technology* 23(1), 313-328. DOI: 10.22069/JWFST.2017.11309.1601
- Pandey, K. K. (2005). "A note on the influence of extractives on the photo-discoloration and photodegradation of wood," *Polymer Degradation and Stability* 87(2), 375-379. DOI: 10.1016/j.polymdegradstab.2004.09.007
- Pandey, K. K., and Pitman, A. J. (2003). "FTIR studies of the changes in wood chemistry following decay by brown-rot and white-rot fungi," *International Biodeterioration & Biodegradation* 52(3), 151-160. DOI: 10.1016/S0964-8305(03)00052-0
- Park, S., Baker, J. O., Himmel, M. E., Parilla, P. A., and Johnson, D. K. (2010). "Cellulose crystallinity index: Measurement techniques and their impact on interpreting cellulase performance," *Biotechnology for Biofuels* 3, 1-10. DOI: 10.1186/1754-6834-3-10
- Pedersen, N. B., Łucejko, J. J., Modugno, F., and Björdal, C. (2021). "Correlation between bacterial decay and chemical changes in waterlogged archaeological wood analysed by light microscopy and Py-GC/MS," *Holzforschung* 75(7), 635-645. DOI: 10.1515/hf-2020-0153
- Philokyprou, M., and Michael, A. (2020). "Environmental sustainability in the conservation of vernacular architecture. The case of rural and urban traditional settlements in Cyprus," *International Journal of Architectural Heritage* 15(11), 1741-1763. DOI: 10.1080/15583058.2020.1719235
- Popescu, C. M., Lisa, G., Manoliu, A., Gradinariu, P., and Vasile, C. (2010). "Thermogravimetric analysis of fungus-degraded lime wood," *Carbohydrate Polymers* 80(1), 78-83. DOI: 10.1016/j.carbpol.2009.10.058
- Pucetaite, M. (2012). *Archaeological Wood from the Swedish Warship Vasa Studied by Infrared Microscopy*, Master Thesis, Lund University Press, Lund, Sweden.
- Reinprecht, L. (2016). *Wood Deterioration, Protection and Maintenance*, John Wiley Sons, Ltd., Chichester, UK.
- Schwanninger, M., Rodrigues, J. C., Pereira, H., and Hinterstoisser, B. (2004). "Effects of short-time vibratory ball milling on the shape of FT-IR spectra of wood and cellulose," *Vibrational Spectroscopy* 36(1), 23-40. DOI: 10.1016/j.vibspec.2004.02.003
- Shimur, R., Nishiok, A., Kano, I., Kod, T., and Nishio, T. (2014). "Novel method for producing amorphous cellulose only by milling," *Carbohydrate Polymers* 102, 645-648. DOI: 10.1016/j.carbpol.2013.11.014

- Skreiberg, A., Skreiberg, Ø., Sandquist, J., and Sørum, L. (2011). “TGA and macro-TGA characterisation of biomass fuels and fuel mixtures,” *Fuel* 90, 2182-2197. DOI: 10.1016/j.fuel.2011.02.012
- Tayla, H. (2007). *Geleneksel Türk Mimarisinde Yapı Sistem ve Elemanları [Structural Systems and Elements in Traditional Turkish Architecture]*, Vol.II, Istanbul: TAÇ Foundation, Istanbul, Turkey.
- Ürkmez, Ö. (2014). “Eski Çağ’da Maraş ya da Marğaşti Germanicia [In Ancient Times: Maraş or Marğaşti Germanicia],” *KSÜ Sosyal Bilimler Dergisi* 11(2), 67-95.
- Wang, S. Y., and Lin, S. J. (1991). “The effect of outdoor environmental exposure on the main component of woods,” *Mokuzai Gakkaishi* 37(10), 954-963.
- Watkinson, S. C., and Eastwood, D. C. (2012). “*Serpula lacrymans*, wood and buildings,” *Advances in Applied Microbiology* 78, 121-149. DOI: 10.1016/B978-0-12-394805-2.00005-1
- Yıldırım, E., and Kalaycı, A. (2022). “Makedon Krallığının Egemenliğinden (İÖ 334) Roma İmparatorluğuna Kadar (İÖ 27) Maraş ve Çevresi [Maraş and its surroundings from the domination of the Macedonian Kingdom (334 BC) to the Roman Empire (27 BC)],” in: *Maraş Araştırmaları-III*, İ. Solak and S. Alıç (eds.), Palet Press, Konya, Turkey, pp. 9-24.
- Yıldırım, E., and Kalaycı, A. (2023). “Roma İmparatorları Augustus’tan (İÖ 27) Vespasianus Dönemine Kadar (İS 72) Maraş ve Çevresi [Maraş and its surroundings from the reign of Roman emperors from Augustus (27 BC) to Vespasian (72 AD)],” in: *Maraş Araştırmaları-IV*, İ. Solak and S. Alıç (eds.), Palet Press, Konya, Turkey, pp. 27-35.
- Zhou, H., Long, Y., Meng, A., Li, Q., and Zhang, Y. (2013). “The pyrolysis simulation of five biomass species by hemi-cellulose, cellulose and lignin based on thermogravimetric curves,” *Thermochimica Acta* 566, 36-43. DOI: 10.1016/j.tca.2013.04.040

Article submitted: September 27, 2024; Peer review completed: January 18, 2025;  
Revised version received: January 31, 2025; Accepted: February 5, 2025; Published:  
March 17, 2025.

DOI: 10.15376/biores.20.2.3424-3442